Kinetic Modeling of Surface-Initiated Photoiniferter-Mediated Photopolymerization in Presence of Tetraethylthiuram Disulfide

Santosh B. Rahane,[†] S. Michael Kilbey II,[†,‡] and Andrew T. Metters*[,†,§]

Department of Chemical and Biomolecular Engineering and Center for Advanced Engineering Fibers and Films, Clemson University, Clemson, South Carolina 29634, and Department of Bioengineering, Clemson University, Clemson, South Carolina 29634

Received November 12, 2007; Revised Manuscript Received September 1, 2008

ABSTRACT: A rate equation-based kinetic model is developed to investigate the effect of important reaction parameters on surface-initiated photoiniferter-mediated photopolymerization (SI-PMP) of methyl methacrylate. In particular, the effect of incident light intensity and concentration of added deactivating species, tetraethylthiuram disulfide (TED), on the growth kinetics of surface-tethered poly(methyl methacrylate) (PMMA) layers was studied in detail. In accord with experimental results, model predictions suggest that maximum rates of PMMA layer growth observed during initial stages of SI-PMP increase as TED concentration ([TED]) is decreased and as light intensity is increased. Conversely, the maximum thickness of the PMMA layers, which is defined as the thickness at which 99% of the surface-tethered polymer chains are irreversibly terminated, increases as [TED] increases and as light intensity decreases. As light intensity and added deactivator affect the number of propagating surface-tethered radicals, findings from this study delineate strategies for optimizing the formation of surface-tethered PMMA brushes by SI-PMP and creating block copolymer brushes.

Introduction

Controlled radical polymerization (CRP) processes are attractive mainly due to their ability to control polymer molecular weight and synthesize multiblock copolymer architectures.[1] Combining CRP techniques with surface-tethered initiators enables dense homopolymer and block copolymer brushes to be synthesized.[2] CRP techniques such as atom transfer radical polymerization (ATRP),[3−9] nitroxide-mediated free-radical polymerization (NMP),[10−12] reversible addition fragmentation transfer (RAFT)[13,14] and photoiniferter-mediated photopolymerization (PMP)[15−24] all have been used to produce polymer brushes. The ability of these CRP techniques to produce polymers with tailored molecular weight and form multiblock copolymer architectures is a consequence of equilibrium between actively propagating radicals and dormant polymer chains being established and maintained during polymer layer growth. This equilibrium keeps the radical concentration low, minimizing irreversible termination and, in turn, preserving the active chain ends necessary for forming multiblock copolymers.

Owing to certain advantages compared to other living-radical polymerization techniques (for example, ease of achieving spatial and temporal control over layer growth),[22,23] we chose surface-initiated photoiniferter-mediated photopolymerization (SI-PMP) to synthesize poly(methyl methacrylate) (PMMA) brushes. Previously, we showed that without intervention, SI-PMP of methyl methacrylate (MMA) suffers from irreversible termination, leading to cessation of polymerization.[22] As a result, these PMMA layers lack the ability of subsequent reinitiation to create multiblock architectures. Knowing that reinitiation is enabled by preservation of active ends during polymerization, we added a source of deactivating species, tetraethylthiuram disulfide (TED), to the reaction mixture.[23] Of course, adding TED shifts the equilibrium toward the dormant state and slows the growth of the PMMA chains. This slowed growth may be offset by increasing the light intensity, which increases the concentration of actively propagating radicals but also increases the likelihood of termination events. This tradeoff, however, impacts the ability to produce block copolymer brushes upon reinitiation with a second monomer.

To date, the impact of these key factors on the kinetics of chain growth, as manifest in the evolution of layer thickness in SI-PMP processes has not been investigated and, with recent advances in photoiniferter chemistries that yield polymers with low polydispersity index (PDI) values,[25] it becomes even more important to understand the effect of various SI-PMP conditions on kinetics of layer growth. Here we use a kinetic model developed for SI-PMP and parametrized using experimental data from SI-PMP of methyl methacrylate to study the dependence of layer growth kinetics on various photopolymerization conditions, such as light intensity and photoiniferter concentration in the presence or absence of the deactivator, TED.

While there are numerous studies devoted to modeling CRP processes in bulk or solution,[26−33] adaptation and application of models to surface-initiated CRP (SI-CRP) is scarce. As far as we are aware, efforts that aim to simulate SI-CRP processes are limited to Monte Carlo simulations developed by Genzer[34] and simulations using rate-based models of Kim et al.[8] The simulations of Genzer used to investigate SI-CRP (specifically surface-initiated ATRP; SI-ATRP) rely on the probabilities of reaction and motion of polymer chains and apply experimentally available kinetic rate constants obtained for solution-phase ATRP. On the other hand, the simulations developed by Kim et al. take a more traditional approach of simultaneously solving rate equations that describe the individual processes (initiation, propagation, and termination) occurring in SI-ATRP.

The model developed in the present work is specific to SI-PMP by virtue of describing the effects of parameters specific to SI-PMP (for example, light intensity); however, the approach is similar to that of Kim et al.,[8] in that it uses rate equations written to describe individual processes. Additionally, because some of the kinetic rate constants (for example, termination rate constants) can be significantly affected by confinement of polymer chains to surface, analogous to the approach taken by

* Corresponding author.
[†] Department of Chemical and Biomolecular Engineering and Center for Advanced Engineering Fibers and Films, Clemson University.
[‡] Current address: Department of Chemistry, University of Tennessee and Center for Nanophase Materials Sciences, Oak Ridge National Laboratory.
[§] Department of Bioengineering, Clemson University.

10.1021/ma702516w CCC: $40.75
Published on Web 11/25/2008

Kim et al.,[8] the rate constants were obtained by the fitting of the experimental results to the model predictions rather than specifying the values *a priori*. As a result, while the approach is applicable to all photoiniferter chemistries that follow a reaction scheme similar to the one under consideration here, the model developed in this work and used to investigate the effect of TED concentration, light intensity and initial photoiniferter concentration on the kinetics of growth is specific to the formation of PMMA brushes. Nevertheless, the results obtained in this study provide a deeper insight into the SI-PMP process: in addition to simply predicting thickness of PMMA layers as a function of various SI-PMP conditions, the model may be used to predict effects of TED concentration and light intensity on maximum rates of SI-PMP and maximum achievable thickness by SI-PMP (both quantities are defined explicitly later in this paper), and as a result, identify trade-offs in both quantities as SI-PMP conditions are changed. The model framework developed in this work can be easily used to understand and predict SI-PMP behaviors and brush formation as functions of SI-PMP conditions, which otherwise would require a battery of detailed and time-consuming experiments.

Experimental Section

Materials and Methods. Sodium diethyldithiocarbamate (Fluka, 97%) was recrystallized from methanol (Fisher Scientific, 99.9%), and *p*-chlorotrimethoxysilane (Gelest Inc., 95%) was used as received. Methyl methacrylate (MMA, Aldrich, 99%) was dehibited by washing with sodium hydroxide (Alfa Aesar, 97%) solution and water, and distilled under vacuum from CaH_2 (Aldrich, 90−95%) prior to use. Anhydrous toluene (Alfa Aesar, 99.8%), anhydrous tetrahydrofuran (THF, Acros, 99.9%), sulfuric acid (EMD Chemicals Inc., 95−98%), hydrogen peroxide (Sigma, 30% v/v in water) and tetraethylthiuram disulfide (TED) (Sigma, 97%) were all used as received.

Silanized photoiniferter, *N*,*N*-(diethylamino)dithiocarbamoylbenzyl(trimethoxy)silane (SBDC), was synthesized by continuously stirring solutions of sodium diethyldithiocarbamate and *p*-chlorotrimethoxysilane in anhydrous THF for 6 h in dry atmosphere. Because the synthesis, purification and NMR analysis that confirms the structure of SBDC are described in detail in our previous publication,[22] they are not repeated here. Formation and analysis of SAMs of photoiniferter on silicon wafers are also previously described.[22] Briefly, preparation of self-assembled monolayers (SAMs) of SBDC involved cleaning of silicon wafers using "piranha acid" (70% sulfuric acid and 30% of hydrogen peroxide by volume), followed by overnight immersion of the cleaned silicon substrate in a 2 mM SBDC toluene solution. These SAM-modified silicon wafers were ready-to-use after repeated rinsing, sonication in toluene, and drying with a stream of dry nitrogen.

Photopolymerization. Monomer solutions consisting of MMA in anhydrous toluene at 4.68 M were prepared, and then TED was dissolved in those solutions. Solutions having TED concentrations of 0.02 mM, 0.2 mM and 2 mM were made and then transferred to air-free Schlenk tubes, degassed by 4−5 freeze−pump−thaw cycles and finally transferred to a preassembled Teflon reaction cell that contains four SBDC-modified surfaces. The assembly of these reaction cells is fully described in our previous papers.[22,23] It should be noted that the assembly of the reaction cell and transfer of degassed MMA/TED solutions into the reaction cell were carried out in a glovebox where the oxygen level is kept below 1 ppm. Once completely assembled and sealed, the reaction cell is taken out of glovebox and exposed to collimated 365 nm light (EXFO 100W Acticure ultraviolet/visible spot-curing system with 365 nm band-pass filter) at desired light intensities. After photopolymerization, the PMMA-modified silicon wafers are sonicated in toluene for 30−45 min to remove any nonbonded polymer.

Characterization. A Beaglehole Instruments phase-modulated Picometer ellipsometer (He−Ne laser, $\lambda = 632.8$ nm) was used to measure the dry layer thicknesses of the SBDC and PMMA layers. Refractive indices of 1.45 and 1.48 were used for the SAMs of SBDC and tethered PMMA layers, respectively. The ellipsometric angles Ψ and Δ were measured at angles of incidence ranging from 80° to 35° (measurements were made every 1.00 degree), and fit using a Cauchy model (Igor Pro. software package) to obtain the thickness with an accuracy of ± 1 nm. Thickness measurements were taken at five different points on every sample in ambient air.

Model Development and Methods

Formulation of the Model. The overall SI-PMP process that occurs in the presence of TED can be broken down into four individual processes. The particular chemistries used when carrying out SI-PMP of MMA have been described in detail with the help of simple schematics in previous publications.[22,23] Briefly, SI-PMP of MMA in the presence of TED primarily involves the following steps:

(i) reversible activation (termination) of surface-tethered photoiniferter molecule (*N*,*N*-(diethylamino)dithiocarbamoylbenzyl(trimethoxy)silane), forming (recombining) a surface-tethered carbon radical, STR•, and a free dithiocarbamyl radical, DTC•;

(ii) reversible cleavage (termination) of TED to yield two free DTC•;

(iii) irreversible termination of surface-tethered radicals via bimolecular termination; and

(iv) propagation via reaction of a STR• with monomer (MMA) to grow a surface-tethered PMMA chain.

We emphasize here that our previous experimental work on the MMA system suggests that bimolecular termination, rather than chain transfer, is the dominant irreversible termination event.[22] Although STR• can attack TED to create the dormant STR−DTC species and a free DTC•, because [TED] ≪ [MMA] and the concentration of STR• is presumed to be low in controlled (free) radical polymerizations, this reversible reaction is not integrated into the model at this level of sophistication.

Mathematically, the first three reactions can be represented by writing a mole balance for each species involved (eqs 1−4):

$$\frac{d[STR\bullet]}{dt} = k_a'[STR{-}DTC] - k_{t,rev}[STR\bullet][DTC\bullet] - k_t[STR\bullet]^2 \quad (1)$$

$$\frac{d[STR-DTC]}{dt} = -k_a'[STR{-}DTC] + k_{t,rev}[STR\bullet][DTC\bullet] \quad (2)$$

$$\frac{d[DTC\bullet]}{dt} = k_{a,TED}'[TED] - k_{t,TED}[DTC\bullet]^2 + k_a'[STR{-}DTC] - k_{t,rev}[STR\bullet][DTC\bullet] \quad (3)$$

$$\frac{d[TED]}{dt} = -k_{a,TED}'[TED] + k_{t,TED}[DTC\bullet]^2 \quad (4)$$

The propagation reaction is represented in terms of the evolution of PMMA layer thickness, T as a function of exposure time, t:

$$\frac{dT}{dt} = k'k_p[STR\bullet][M] \quad (5)$$

In these equations [STR•] is the concentration of surface-tethered radicals, [M] is monomer concentration, [DTC•] is the concentration of DTC•, [STR−DTC] is the concentration of surface-tethered radicals in deactivated state (made by reversible capping of STR• with DTC•), $k_{a,TED}'$ is the effective kinetic constant for (reversible) activation of surface-tethered photoiniferter molecules into surface-tethered carbon radicals, $k_{t,rev}$ is the kinetic constant for deactivation of STR• by reaction with DTC• (which is a reversible termination), k_t is the kinetic constant for bimolecular termination of STR•, $k_{a,TED}'$ is the effective kinetic constant for activation (cleavage) of TED, $k_{t,TED}$

Table 1. Values of Parameters Used To Simulate the Variation of Thickness as a Function of Time[a]

parameter	value	source
$[STR-DTC]_0$	2×10^{-5} M	parameter estimation
k_a'	0.00152 s^{-1}	eq 6 with $I_0 = 5$ mW/cm^2
$k_{t,rev}$	6.6×10^7 M^{-1} s	parameter estimation
k_t	30×10^9 M^{-1} s	parameter estimation
$k_{a,TED}'$	0.003198 s^{-1}	eq 7 with $I_0 = 5$ mW/cm^2
$k_{t,TED}$	2×10^5 M^{-1} s	Plyusnin et al.[37]
$k'k_p$	14.459×10^6 nm/[M^2 s]	parameter estimation

[a] The values of unknown kinetic parameters, $[STR-DTC]_0$, $k_{t,rev}$, k_t, k', and k_p were obtained by fitting the experimental PMMA layer thicknesses as functions of time at [TED] = 0 and 2×10^{-3} M.

is the kinetic constant for reversible deactivation of dithiocarbamyl radicals to form TED, [TED] is the concentration of TED. In eq 5, k_p is the propagation rate constant and k' is the proportionality constant between the rate of polymerization and growth rate of PMMA layer. It should be noted that the constant, k', implies a proportional relationship between average molecular weight of chains and thickness. This assumption is often made with surface-initiated, controlled (free) radical polymerizations from flat, low area substrates because a sufficient quantity of chains cannot be recovered (after degrafting) to obtain molecular weight (MW) and PDI information on the tethered chains.[22,35,36] While a sufficient amount of polymer can be recovered when high surface area substrates such as silica gel are used, due to solution opacity and nonuniform exposure to initiating sites, MW and PDI data obtained in the case of SI-PMP from silica gel may not accurately represent the chains grown from flat surfaces. For these reasons and because the focus of this paper is on the development and application of a model for simulating the process of SI-PMP, efforts to carry out SI-PMP from silica gel, measure the polymer layer thickness and then subsequently degraft, recover, and characterize the chains to obtain MW and PDI of polymer chains were not made. Nevertheless and as noted previously, a proportional relationship between average molecular weight of polymer chains and thicknesses of polymer layers has been described and justified previously.[22,35,36]

Equations 1−5 when taken together constitute a comprehensive kinetic model for simulating PMMA layer growth as a function of various photopolymerization conditions. Application of the described model to characterize the kinetics of SI-PMP, however, requires an understanding of its inherent assumptions and limitations, as well as suitable values for the unknown kinetic parameters.

Parameterizing the Model. The values of k_a' and $k_{a,\mathrm{TED}}'$ are calculated using eqs 6 and 7,[37] respectively, and are listed in Table 1.

$$k_a' = f_1 k_a = \frac{f_1 I_0 \varepsilon_P \lambda}{N_{AV} h c} \tag{6}$$

$$k_{a,\mathrm{TED}}' = f_2 k_{a,\mathrm{TED}} = \frac{f_2 I_0 \varepsilon_{\mathrm{TED}} \lambda}{N_{AV} h c} \tag{7}$$

In these expressions, I_0 is the light intensity (in mW/cm^2), ε_P is the extinction coefficient of photoiniferter molecules, $\varepsilon_{\mathrm{TED}}$ is the extinction coefficient of TED, λ is the wavelength of incident UV-light (365 nm), N_{AV} is Avogadro's number, h is Planck's constant and c is the speed of light. For our simulations, ε_P and $\varepsilon_{\mathrm{TED}}$ are calculated using spectral absorbance data for photoiniferter and TED molecules, respectively (ε_P=100 M^{-1} cm^{-1} and $\varepsilon_{\mathrm{TED}} = 210$ M^{-1} cm^{-1} at 365nm[38]). The effective activation constants, k_a' and $k_{a,\mathrm{TED}}'$ are expressed as the product of the corresponding initiator efficiencies, f_1 and f_2, and the activation kinetic constants for photoiniferter (k_a) and TED ($k_{a,\mathrm{TED}}$). Close analysis of eqs 1−4 and eqs 6−7 reveals that changes in f_1 and f_2 will affect the kinetics of PMMA layer growth in the same fashion as changes in k_a and $k_{a,TED}$, respectively. Furthermore, a change in the value of initiator efficiency can be offset by a corresponding change in the activation kinetic constant without changing the effective activation kinetic constant. Because it is not possible to decouple variations in initiator efficiencies from those of the activation kinetic constants, values of f_1 and f_2 were assumed to be 1 to reduce the number of unknown variables. The value of $k_{t,\mathrm{TED}}$ was obtained from literature.[39]

Because of confinement of the photoiniferter and PMMA chains to the surface, the values of the remaining kinetic constants, $k_{t,rev}$, k_t, k', k_p and, initial concentration of surface-tethered photoiniferter molecules, $[STR-DTC]_0$, are expected to differ significantly from parameter values available in the literature for free-radical polymerization of bulk or highly cross-linked samples. Therefore, as indicated in Table 1 and described in detail later, these values were obtained by fitting model predictions with the experimental PMMA layer thicknesses measured using multiangle ellipsometry. For example, the value for k_t found by model fitting and listed in Table 1 (3×10^{10} M^{-1} s) is larger than typical values ($\sim 10^7$ M^{-1} s^{-1}) reported for bulk free-radical polymerizations of PMMA by a few orders of magnitude, but is in agreement with the value of k_t reported for polymerizations in low-viscosity media.[37] With this in mind and given the process used to obtain the unknown kinetic constants by fitting the data, the value of k_t reported in Table 1 is not unreasonable and, as described in detail later, is sufficiently accurate to predict correctly the trends observed in the experimental data.

Model Assumptions and Limitations. The following assumptions were made in developing the kinetic model embodied in eqs 1−5:

(1) Differences in the chemical structures of the surface-attached photoiniferter molecule and dithioester end groups of the reversibly deactivated polymer chains are assumed to not alter the initiation/reinitiation kinetics. The analogous assumption has been previously made in modeling of ATRP.[26,27,29]

(2) The proportionality constant, k' in eq 5 relates photopolymerization rate to the overall growth of polymer brush layer.[35,36] Although k' depends on the grafting density of the polymer brush, which ostensibly is a complex function of photopolymerization conditions, in the current model k' is assumed to be constant for all photopolymerization conditions examined herein.

3) Monomer concentration is assumed to be constant for SI-PMP. This assumption is often employed when describing SI-CRP from low surface-area substrates.[4,8,40,41]

Methods. All simulations were carried out on a Dell (Pentium-4) platform using commercially available Polymath (Version 5.0) software. The "STIFF" algorithm, based on Rosenbrock methods,[42] was used to solve the differential equations simultaneously.

Results and Discussion

Estimation of Unknown Kinetic Parameters and Validation of Kinetic Model. The values of unknown kinetic parameters, $[STR-DTC]_0$, $k_{t,rev}$, k_t, k', and k_p were obtained by fitting the model to the experimental PMMA layer thicknesses as functions of time at [TED] = 0 and 2×10^{-3} M (lowest and highest experimental [TED] investigated in these studies). This data-fitting procedure involved optimization of unknown kinetic parameters such that the mean-squared error between the experimental data and model predictions were minimized. The kinetic parameters obtained by fitting are listed in Table 1 along with the values of parameters specified *a priori*. These parameters were then used to simulate the growth of PMMA layers as a function of time at [TED] = 0, 2×10^{-5}, 2×10^{-4} and 2×10^{-3} M.

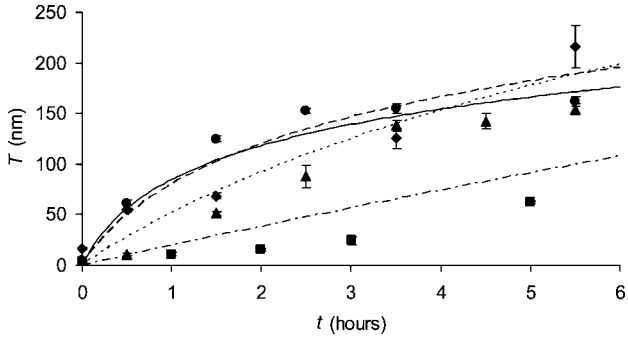

Figure 1. Comparison of time-dependent experimental and simulated PMMA layer thicknesses synthesized at various TED concentrations. The symbols represent the experimental data while the lines are results obtained via simulation. Concentrations of TED in toluene were 0 M (●; continuous line), 2×10^{-5} M (◆; dashed line), 2×10^{-4} M (▲; dotted line) and 2×10^{-3} M (■; dashed-dotted line). [MMA] = 4.68 M in toluene and light intensity = 5 mW/cm^2 at 365nm.

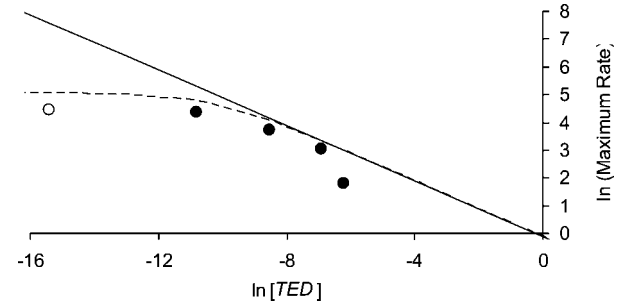

Figure 2. Comparison of experimentally observed maximum growth rates (●) as a function of TED concentration with predicted values based on the full kinetic simulation (broken line) and a simplified kinetic model (thin solid line) using the pseudosteady state assumption. The hollow circle (○) represents the experimental case of [TED] = 0 M. On logarithmic scale, for [TED] $\geq 2 \times 10^{-5}$ M, the slope of predicted maximum rate versus [TED] is $-1/2$ indicating that the theoretical maximum growth rate for the PMMA layers scales with $[TED]^{-1/2}$.

Figure 1 shows experimental results that capture the effect of [TED] on the growth of PMMA layers as a function of time and their comparison with the simulated time-dependent PMMA layer thickness profiles. It should be noted that the time axis for each [TED] has been shifted to exclude the experimentally observed initial lag period, where slow PMMA layer growth is seen. This slow growth/initial lag period has been previously attributed to PMMA layer growth within the "mushroom" regime,[22] but it could also be due to rapid termination of iniferter molecules at the beginning of the photopolymerization.[43] Complete thickness profiles that include experimental data within the initial lag periods are presented in our previous publications.[22,23]

As can be seen from Figure 1, though the simulated PMMA layer thickness profiles do not match exactly with the experimental data, the important trends in PMMA layer thickness as a function of time are correctly predicted using the described model, thereby validating the described simulation strategy. Notably, the model predicts crossovers that are observed experimentally: at [TED] = 2×10^{-5} M, the thickness of the PMMA layer after 6 h of exposure (209 ± 5 nm) exceeds that of the sample polymerized without TED (162 ± 4 nm). Additionally, as shown in Figure 2, the model also correctly predicts the experimentally observed decrease in the maximum PMMA layer growth rate with increasing [TED].

The described model and simulation strategy are also validated by comparing predictions of maximum PMMA layer growth rates of the full model with predictions resulting from a simpler, pseudosteady state model that is applicable during the initial stages of SI-PMP when PMMA layer growth rate is at its maximum. The pseudosteady state model (complete derivation provided as Supporting Information) is developed by simplifying the comprehensive model (eqs 1−5) according to following assumptions:

(1) Irreversible termination reactions are negligible;

(2) Pseudosteady state is assumed for surface-tethered radicals and deactivating DTC• radicals in solution;

(3) [TED] is in considerable excess compared to $[STR-DTC]_0$ (the initial concentration of surface-tethered photoiniferter molecules); and

(4) TED activation is small such that [TED] is equal to its initial value, $[TED]_0$.

Applying these assumptions produces the following expression for the concentration of surface-tethered radicals at pseudosteady state, $[STR\bullet]_s$.

$$[STR\bullet]_s = \frac{k_a'[STR-DTC]_0}{k_a' + \sqrt{\frac{k_{a,TED}'[TED]_0}{k_{t,TED}}}} \quad (8)$$

This expression for $[STR\bullet]_s$ can be substituted into eq 5 to obtain the (maximum) growth rate of the PMMA layers. Equation 8 suggests that $[STR\bullet]_s$ and, therefore, the maximum growth rate of PMMA layers, decreases with $[TED]_0^{1/2}$ when TED is in excess and activation is minimal (assumptions 3 and 4). Figure 2 compares the experimentally obtained maximum rates with the maximum rates obtained from simulations and predictions of pseudosteady state model (eq 8) as a function of $[TED]_0$. The maximum rates from experimental results[23] were obtained from the slope of a straight line plotted through the first two data points for thickness of PMMA layers in brush regime. Similarly, to obtain the simulated maximum rates, thicknesses at $t = 0.0$ h and $t = 0.012$ h were used. As can be seen from Figure 2, in the region of excess TED (for our experimental system, [TED] $\geq 2 \times 10^{-5}$ M), the simulated maximum rates and maximum rates predicted using pseudosteady state model agree with one another and decrease inversely with $[TED]_0^{1/2}$. In addition, both the comprehensive and pseudosteady state model predictions agree reasonably well with the experimentally obtained maximum PMMA layer growth rates at higher [TED] values. However, only the simulations based on the full kinetic model are also able to predict the experimentally observed plateau in PMMA layer growth rate that occurs at diminishingly small [TED] values. These features further validate described model and simulation strategy. The deviation of model predictions from the experimental data at high [TED] values (e.g., [TED] = 2×10^{-3} M) is likely due to two reasons: (i) lower light intensity at the site of surface polymerization due to significant light absorption by TED in solution and (ii) monomer consumption *via* dithiocarbamyl radical-initiated polymerization in solution, which can be significant at high monomer concentrations.[23]

Effect of [TED] on PMMA Layer Growth. The observed decrease in maximum (initial) growth rates with increasing [TED] is a consequence of a decrease in the initial, instantaneous concentration of propagating surface-tethered radicals, which is brought about by a shift in the equilibrium between actively propagating radicals and dormant PMMA chains toward the dormant state. With the aid of the kinetic simulations, this equilibrium shift can be observed through changes in the surface-tethered radical concentration ([STR•]), which greatly impacts overall polymerization behavior. For the sake of brevity, the changes in these actively propagating radicals as a function of various SI-PMP parameters are not presented here. In addition

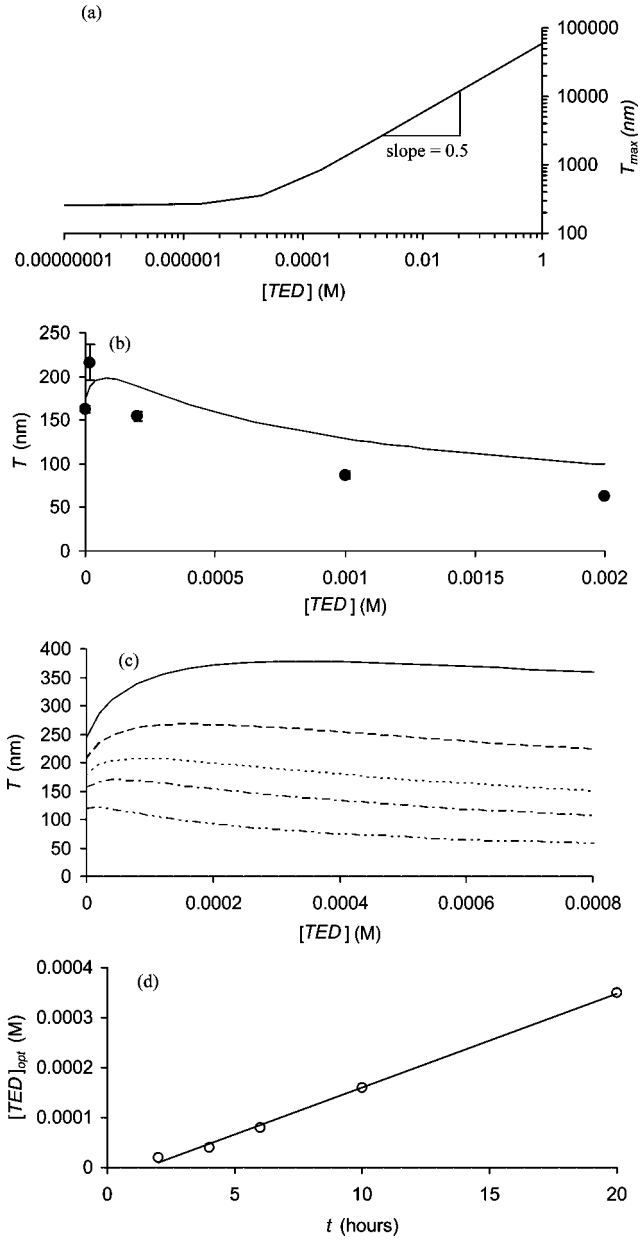

Figure 3. (a) Simulated maximum PMMA layer thickness as a function of TED concentration. The light intensity used in the simulations is 5 mW/cm^2. The maximum thicknesses at all [TED] are defined as when 99% of surface-tethered initiator sites are irreversibly terminated. (b) Comparison of experimental (filled circles) and simulated (continuous line) PMMA layer thicknesses at various TED concentrations. Exposure time = 5.5 h and light intensity = 5 mW/cm^2. (c) Evolution of simulated PMMA layer thickness as a function of TED concentration at various exposure times, using I_0 = 5mW/cm^2. The exposure times of 2 h (dashed double-dotted line), 4 h (dashed-dotted line), 6 h (dotted line), 10 h (broken line), and 20 h (continuous line) are shown. (d) Predicted optimum [TED] that maximizes thickness as a function of exposure time. The hollow circles (○) represent the simulated $[TED]_{opt}$ extracted from part c and the thin solid line ($[TED]_{opt} = 2 \times 10^{-5}t - 3 \times 10^{-5}$) is a best fit to $[TED]_{opt}$ as a function of exposure time (t).

to a decrease in propagation rate (growth rate), the decrease in the concentration of the actively propagating radicals also results in a decrease in irreversible termination reactions.[26,44] By virtue of this decrease in irreversible termination reactions with increasing [TED], the average lifetime of growing PMMA chains increases with [TED]. As a result, the maximum theoretical thickness, T_{max}, achievable by SI-PMP also increases with [TED] as shown in Figure 3a. T_{max} in this figure is defined as the thickness at which 99% of the tethered polymer chains are irreversibly terminated. As shown in Figure 3a, while T_{max} is approximately independent of [TED] at concentrations less than $[STR-DTC]_0$, for [TED] > $[STR-DTC]_0$, where dithiocarbamyl radicals generated from TED are in excess of those generated from surface-tethered photoiniferter, T_{max} is proportional to $[TED]^{1/2}$. While T_{max} increases with [TED], the square root relationship between T_{max} and [TED] implies that the effectiveness of adding TED to increase T_{max} decreases at higher TED concentrations. Therefore, it may not be feasible to simply increase [TED] to increase T_{max} above certain thicknesses. It should also be noted that the exposure time required to reach T_{max} also increases with [TED]. These increases in T_{max} and required exposure time, both of which occur with increasing [TED], are consequences of the previously noted tradeoff between decreasing rates of surface-tethered chain propagation and irreversible termination.

A decrease in irreversible termination with increasing [TED] also explains the crossover observed in experiments and simulations: after a certain exposure time, the thickness of PMMA layers synthesized in presence of TED exceeds the thickness of PMMA layers synthesized without TED or at lower [TED] because TED enables continued layer growth by virtue of mitigating irreversible termination. This leads to the realization that for a given exposure time, there should be an optimum [TED] that maximizes PMMA layer thickness. Figure 3b compares the experimentally observed and simulated PMMA layer thicknesses at various [TED] after 5.5 h. As can be seen in Figure 3b, both experimental data and simulations indicate an optimum [TED] that produces a maximum in PMMA layer thickness at the noted polymerization time. This observation of an optimum [TED] is analogous to reports of an optimum catalyst concentration that yields maximum polymer layer thickness for surface-initiated ATRP of methyl acrylate.[8]

Because the equilibrium between actively propagating radicals and dormant polymer chains as well as the tradeoff between propagation and irreversible termination rates are shifted by [TED], the optimum TED concentration that yields maximum PMMA layer thickness, $[TED]_{opt}$, also should vary with the polymerization time. Figure 3c shows the simulated PMMA layer thicknesses as a function of [TED] at various polymerization times. As shown in Figure 3d, $[TED]_{opt}$ increases linearly with polymerization time and the slope is approximately equal to the value of $[STR-DTC]_0$ (2×10^{-5} M) used in the simulations.

Effect of Light Intensity on PMMA Layer Growth Kinetics. The previous section demonstrates how the preaddition of TED impacts PMMA layer growth by affecting the equilibrium between actively propagating radicals and dormant PMMA chains. Alternatively, this equilibrium can also be affected by manipulating the activation constant, k_a', *via* changes in light intensity. To investigate how light intensity affects PMMA layer growth, additional experiments and simulations were performed where light intensity was varied while keeping [TED] and [M] constant.

Using experimental data and results from simulations, Figure 4a shows the effect of light intensity on PMMA layer growth. The PMMA layer growth at I_0 = 5 mW/cm^2 matches the simulated PMMA layer growth very well, which is expected because the model parameters used to simulate layer growth are obtained from best fits of these data at this I_0. However, the model overpredicts layer growth at 2 mW/cm^2. One obvious reason for this overprediction is because the proportionality constant k' that relates the molecular weight of PMMA chains with the observed layer thickness varies with grafting density. Because grafting density and in turn, layer thickness is impacted by light intensity,[45] the value of k' obtained by fitting the experimental thicknesses to the model predictions at one

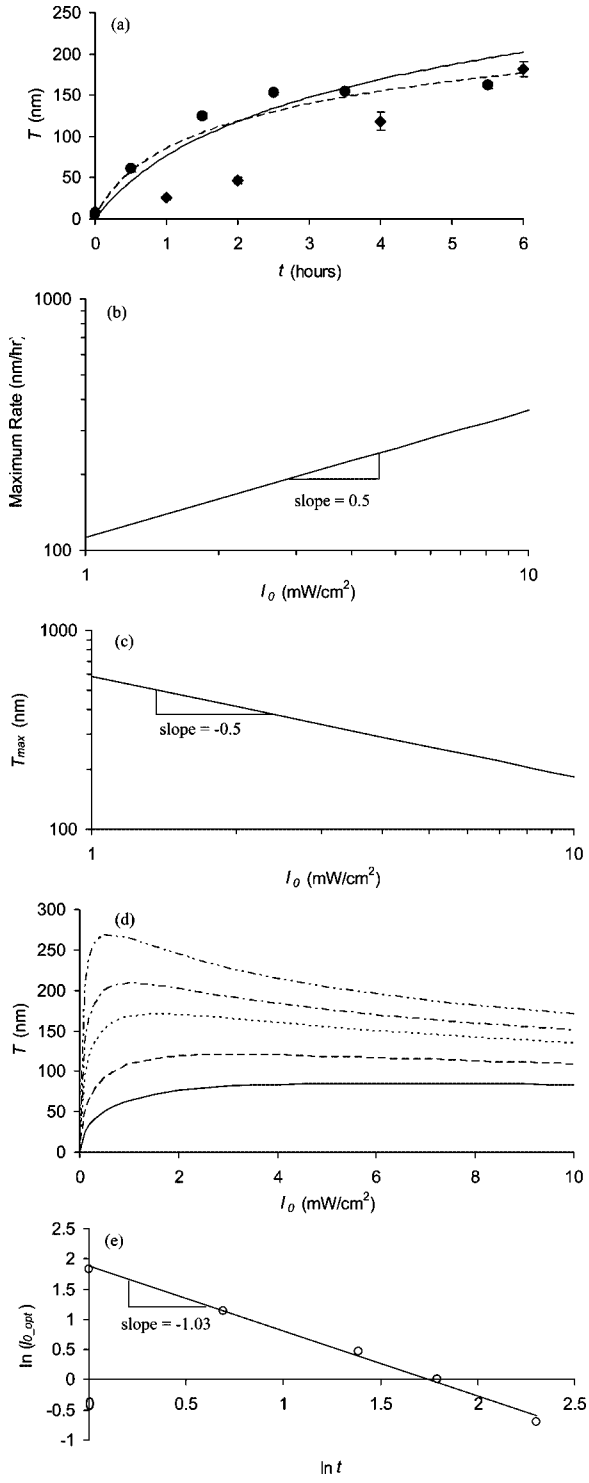

Figure 4. (a) Comparison of time-dependent experimental (data points) and simulated (lines) PMMA layer thicknesses synthesized at various light intensities: 2 mW/cm^2 (◆; thin line) and 5 mW/cm^2 (●; broken line). (b) Simulated maximum growth rates for PMMA layers as a function of light intensity. (c) Simulated maximum PMMA layer thickness as a function of light intensity. The maximum thicknesses are defined as the thickness at which 99% of the surface-tethered initiator sites are irreversibly terminated. (d) Evolution of simulated PMMA layer thickness as a function of light intensity at various exposure times: 1 h (continuous line), 2 h (broken line), 4 h (dotted line), 6 h (dashed-dotted line) and 10 h (dashed double-dotted line). No TED was present. e) Optimum light intensity that maximizes layer thickness as a function of exposure time. No TED was present. The hollow circles represent the simulated I_{0_opt} obtained from Figure 4d and the thin solid line ($\ln I_{0\_opt} = -1.03 \ln t + 1.88$) is a best-fit to I_{0_opt} as a function of exposure time, t.

intensity value cannot be used for rigorous tests of behavior at other intensities. Nevertheless, the trends observed in the experimental thickness data as a function of time are qualitatively predicted using the kinetic model. Both experimental results and simulations indicate that the maximum PMMA layer growth rate observed during the initial stages of SI-PMP increases with light intensity. Furthermore, in the latter stages of polymerization, the thickness of a PMMA layer grown at lower intensity exceeds the thickness of a similar layer grown at higher intensity.

In a fashion similar to the analysis of the effect of [TED] on PMMA layer growth, the effect of light intensity can be understood by studying its effect on the (i) maximum growth rate during the initial stages of polymerization, (ii) maximum layer thickness, and (iii) crossover of thickness versus time profiles. Figure 4b shows the effect of light intensity on maximum growth rate on a logarithmic scale. On a log−log plot, the predicted maximum growth rate increases with incident light intensity with a slope of approximately 0.5, indicating that the maximum growth rate is proportional to $I_0^{1/2}$. This square-root dependence of maximum growth rate on light intensity is consistent with our previously developed model employing bimolecular termination as the dominant termination mechanism, which also suggests a square root dependence of initial surface-tethered radical concentration on light intensity.[22] Conversely, as shown in Figure 4c, the maximum PMMA layer thickness, T_{max} (defined as the thickness at which 99% of the tethered polymer chains are irreversibly terminated), is inversely proportional to $I_0^{1/2}$.

Analogous yet opposite to the effect of [TED] on PMMA layer growth, the effect of light intensity on maximum growth rate and maximum thickness is again a consequence of the tradeoff between propagation and irreversible termination reactions. As a result of this tradeoff, for a given polymerization time there exists an optimum light intensity (I_{0_opt}) that maximizes PMMA layer thickness (Figure 4d). This observation of optimum light intensity is in agreement with the previously obtained results of surface-initiated UV-light induced radical polymerization of styrene.[45] To understand the impacts and trade-offs associated with the observation of an optimum light intensity, it is instructive to consider the fact that increases in polymer layer thickness are consequences of increases in both grafting density and average chain molecular weight. At light intensities lower than I_{0_opt}, the concentration of actively propagating radicals increases as light intensity is increased, and in turn, the layer thickness increases by the virtue of increase in grafting density. For light intensities above I_{0_opt}, the concentration of propagating radicals is sufficiently high that there is a significant number of bimolecular termination reactions occurring, which limits the average molecular weight of polymer chains and polymer layer thickness.

The fact that these competing events are time-dependent leads to the conclusion that I_{0_opt} is also time-dependent: It will take longer at lower light intensities than at higher light intensities to reach the stage where irreversible termination reactions dominate because buildup of propagating radicals is slower. In other words, as exposure time is increased, I_{0_opt} should decrease. Predictions in Figure 4e show that I_{0_opt} is inversely related to exposure time.

In summary, in terms of maximum growth rate, maximum achievable thickness and crossover of thicknesses, increases in [TED] and decreases in incident light intensity affect SI-PMP kinetics in a similar fashion. However, it should be noted that the mechanisms involved in these two cases are inherently different: while increases in [TED] slow down the free-radical propagation rate by reversibly terminating actively growing chain ends, decreases in light intensity decrease the rate of

initiation and therefore the concentration of propagating radicals generated per unit time. Though this mechanistic difference is irrelevant to the kinetics of layer growth, it is crucial to emphasize that this will have strong influence on the reinitiation ability of polymer layers and the structure of block copolymer layers formed upon reinitiation. This subject is the focus of our current modeling efforts.

Conclusions

Without *a priori* determination of all kinetic parameters, the model developed in this work is incapable of predicting absolute values for critical polymer brush properties such as instantaneous thickness and growth rate. However, the trends and sensitivities to various reaction parameters predicted by this rate-based model are reasonably accurate and therefore, within its limitations, the described model constitutes a useful tool for studying the ability to efficiently synthesize well-defined polymer brushes by SI-PMP. Specifically, the kinetic model developed in this work provides significant insight into surface-initiated photoiniferter-mediated photopolymerization of MMA. Buttressed by experimental results, model predictions indicate that increasing [TED] and decreasing light intensity impact PMMA layer growth in similar fashions through distinctly different mechanisms. While the maximum layer growth rate observed during the initial stages of SI-PMP is inversely proportional to $[TED]_0^{1/2}$ and proportional to $I_0^{1/2}$, the maximum achievable thickness is proportional to $[TED]_0^{1/2}$ and inversely proportional to $I_0^{1/2}$. These tradeoffs between maximum layer growth rate and maximum achievable thickness are consequences of the relationship between reversible and irreversible termination in the SI-PMP system. These termination events are coupled to one another through the equilibrium that is rapidly established between actively propagating and dormant PMMA chains and readily affected by [TED] and I_0. As a result of these somewhat complex interrelationships, there exists an optimum [TED] and optimum I_0 that yield a polymer brush with maximum thickness for a given exposure time. Thus, the conditions used to grow the tethered PMMA layer have significant implications on the rate and total extent of layer growth: increasing I_0 and decreasing [TED] does not necessarily maximize layer thickness for a given polymerization condition or reaction time. Finally, while [TED] and I_0 affect the kinetics of polymer layer growth in a similar, yet opposite manner, their impact on the structure and reinitiation ability of the resulting polymer layers is very different. Investigating these differences and adding more complexity to the model (for example, adding alternate reactions such as chain transfer to TED to yield STR-DTC and a free dithiocarbamyl radical[46]) is the focus of future modeling efforts.

Acknowledgment. We gratefully acknowledge the Center for Advanced Engineering Fibers and Films (CAEFF) for financial support under the Engineering Research Centers Program (NSF Award Number EEC-9731680). SMKII acknowledges with thanks the stimulating environment of the Center for Nanophase Materials Sciences a DOE Office of Science supported user facility at Oak Ridge National Laboratory, which fostered completion of this work during a sabbatical period.

Supporting Information Available: Text giving a derivation of the pseudo-steady state model. This material is available free of charge via the Internet at http://pubs.acs.org.

References and Notes

(1) Matyjaszewski, K. Comparison and Classification of Controlled/Living Radical Polymerizations. In *Controlled/Living Radical Polymerization: Advances in ATRP, NMP and RAFT*; Matyjaszewski, K., Eds.; ACS Symposium Series 768; American Chemical Society: Washington, DC, 2000; p 2−26.
(2) Zhao, B.; Brittain, W. J. *Prog. Polym. Sci.* **2000**, *25*, 677–710.
(3) Ejaz, M.; Yamamoto, S.; Ohno, K.; Tsujii, Y.; Fukuda, T. *Macromolecules* **1998**, *31*, 5934–5936.
(4) Matyjaszewski, K.; Miller, P. J.; Shukla, N.; Immaraporn, B.; Gelman, A.; Luokala, B. B.; Siclovan, T. M.; Kickelbick, G.; Vallant, T.; Hoffmann, H.; Pakula, T. *Macromolecules* **1999**, *32*, 8716–8724.
(5) Zhao, B.; Brittain, W. J. *Macromolecules* **2000**, *33*, 8813–8820.
(6) Shah, R. R.; Merreceyes, D.; Husemann, M.; Rees, I.; Abbott, N. L.; Hawker, C. J.; Hedrick, J. L. *Macromolecules* **2000**, *33*, 597–605.
(7) Ejaz, M.; Tsujii, Y.; Fukuda, T. *Polymer* **2001**, *42*, 6811–6815.
(8) Kim, J. B.; Huang, W.; Miller, M. D.; Baker, G. L.; Bruening, M. L. *J. Polym. Sci. Part A: Poly. Chem.* **2003**, *41*, 386–394.
(9) Boyes, S. G.; Granville, A. M.; Baum, M.; Akgun, B.; Mirous, B. K.; Brittain, W. J. *Surf. Sci.* **2004**, *570*, 1–12.
(10) Husseman, M.; Malmström, E. E.; McNamara, M.; Mate, M.; Mecerreyes, D.; Benoit, D. G.; Hedrik, J. L.; Mansky, P.; Huang, E.; Russell, T. P.; Hawker, C. J. *Macromolecules* **1999**, *32*, 1424–1431.
(11) Husemann, M.; Morrison, M.; Benoit, D.; Frommer, J.; Mate, C. M.; Hingsberg, W. D.; Hedrik, J. L.; Hawker, C. J. *J. Am. Chem. Soc.* **2000**, *122*, 1844–1845.
(12) Bartholome, C.; Beyou, E.; Bourgeat-Lami, E.; Chaumont, P.; Zydowicz, N. *Macromolecules* **2003**, *36*, 7946–7952.
(13) Tsujii, Y.; Ejaz, M.; Sato, K.; Goto, A.; Fukuda, T. *Macromolecules* **2001**, *34*, 8872–8878.
(14) Baum, M.; Brittain, W. J. *Macromolecules* **2002**, *35*, 610–615.
(15) Nakayama, Y.; Matsuda, T. *Macromolecules* **1996**, *29*, 8622–8630.
(16) Luo, N.; Metters, A. T.; Hutchison, J. B.; Bowman, C. N.; Anseth, K. S. *Macromolecules* **2003**, *36*, 6739–6745.
(17) Higashi, J.; Nakayama, Y.; Marchant, R. E.; Matsuda, T. *Langmuir* **1999**, *15*, 2080–2088.
(18) Kobayashi, T.; Takahashi, S.; Fujii, N. *J. Appl. Polym. Sci.* **1993**, *49*, 417–423.
(19) de Boer, B.; Simon, H. K.; Werts, M. P. L.; van der Vegte, E. W.; Hadziioannou, G. *Macromolecules* **2000**, *33*, 349–356.
(20) Qin, S. H.; Qiu, K. Y. *Eur. Poly. J.* **2001**, *37*, 711–717.
(21) Nakayama, Y.; Matsuda, T. *Macromolecules* **1999**, *32*, 5405–5410.
(22) Rahane, S. B.; Kilbey, S. M., II.; Metters, A. T. *Macromolecules* **2005**, *38*, 8202–8210.
(23) Rahane, S. B.; Metters, A. T.; Kilbey, S. M., II. *Macromolecules* **2006**, *39*, 8987–8991.
(24) Rahane, S. B.; Floyd, J. A.; Metters, A. T.; Kilbey, S. M. *II Adv. Funct. Mater.* **2008**, *18*, 1232–1240.
(25) Lalevée, J.; Blanchard, N.; El-Roz, M.; Allonas, X.; Fouassier, J. P. *Macromolecules* **2008**, *41*, 2347–2352.
(26) Fischer, H. *Macromolecules* **1997**, *30*, 5666–5672.
(27) Fischer, H. *J. Polym. Sci., Part A: Polym. Chem.* **1999**, *37*, 1885–1901.
(28) Butté, A.; Storti, G.; Morbidelli, M. *Chem. Eng. Sci.* **1999**, *54*, 3225–3231.
(29) Zhu, S. *Macromol. Theory Simul.* **1999**, *8*, 29–37.
(30) He, J.; Li, L.; Yang, Y. *Macromol. Theory Simul.* **2000**, *9*, 463–468.
(31) Zhang, M.; Ray, W. H. *J. Appll. Polym. Sci.* **2002**, *86*, 1630–1662.
(32) Wang, A. R.; Zhu, S. *J. Polym. Sci., Part A: Polym. Chem.* **2003**, *41*, 1553–1566.
(33) Wang, A. R.; Zhu, S. *Macromol. Theory Simul.* **2003**, *12*, 663–668.
(34) Genzer, J. *Macromolecules* **2006**, *39*, 7157–7169.
(35) Sankhe, A. Y.; Husson, S. M.; Kilbey, S. M., II. *J. Polym. Sci., Part A: Polym. Chem.* **2007**, *45*, 566–575.
(36) Harris, B. P.; Metters, A. T. *Macromolecules* **2006**, *39*, 2764–2772.
(37) Odian, G. *Principles of Polymerization*, 4th ed.; John Wiley & Sons: Hoboken, NJ, 2004.
(38) Lovell, L. G.; Elliott, B. J.; Brown, J. R.; Bowman, C. N. *Polymer* **2001**, *42*, 421–429.
(39) Plyusnin, V. F.; Kuznetzova, E. P.; Bogdanchikov, G. A.; Grivin, V. P.; Kirichenko, V. N.; Larionov, S. V. *J. Photochem. Photobiol. A: Chem.* **1992**, *68*, 299–308.
(40) Sankhe, A. Y.; Husson, S. M.; Kilbey, S. M., II. *Macromolecules* **2006**, *39*, 1376–1383.
(41) Gopireddy, D.; Husson, S. M. *Macromolecules* **2002**, *35*, 4218–4221.
(42) Hairer, E.; Wanner, G. Solving Ordinary Differential Equations II: *Stiff and Differential-Algebraic Problems*, 2nd ed.; Springer-Verlag: Berlin, Germany, 2002, Chapter IV.7, pp 102−117.
(43) Bao, Z.; Bruening, M. L.; Baker, G. L. *Macromolecules* **2006**, *39*, 5251–5258.
(44) Doi, T.; Matsumoto, A.; Otsu, T. *J. Polym. Sci., Part A: Polym. Chem.* **1994**, *32*, 2911–2918.
(45) Prucker, O.; Schimmel, M.; Tovar, G.; Knoll, W.; Rühe, J. *Adv. Mater.* **1998**, *10*, 1073–1077.
(46) Kilambi, H.; Reddy, S. K.; Bowman, C. N. *Macromolecules* **2007**, *40*, 6131–6135.

MA702516W